



J. Dairy Sci. TBC

<https://doi.org/10.3168/jds.2024-24678>

© TBC, The Authors. Published by Elsevier Inc. on behalf of the American Dairy Science Association®.
This is an open access article under the CC BY license (<http://creativecommons.org/licenses/by/4.0/>).

Carry-over effects of maternal late-gestation heat stress on granddaughter's growth and mammary gland development

Grace. A. Larsen and Jimena Laporta*

Department of Animal and Dairy Sciences, University of Wisconsin-Madison, WI, USA, 53706

ABSTRACT

Maternal (F_0) exposure to late-gestation heat stress reduces their daughter's (F_1) mammary gland fat pad mass (FP), parenchyma (PAR) mass, and epithelial cell proliferation when evaluated at birth and weaning, and go on to produce less milk in their first lactation. Herein, we investigated the effect of maternal late-gestation heat stress on whole-body growth and mammary development of their granddaughters (F_2). Multiparous F_0 cows had access to heat abatement ($n = 41$, shade, and active cooling via fans and water soakers) or not ($n = 41$, shade only) for the last 56 d of gestation during a subtropical summer. Consequently, the F_1 daughters, born to F_0 cows, were heat-stressed (HT_{F1} , $n = 36$) or cooled (CL_{F1} , $n = 37$) in utero during the last 2 mo of gestation. All F_1 heifers were raised as an identically managed cohort until first calving. The F_2 granddaughters, born to HT_{F1} (HT_{F2} , $n = 12$) or CL_{F1} (CL_{F2} , $n = 17$), were raised as an identically managed cohort until 70 d of age. Dry matter intake (DMI), body weight, hip height, wither height, chest girth, head circumference, mammary gland teat length, and left-right and front-rear teat distances were measured. Average daily gain (ADG) was calculated for the pre-weaned period (0–49 d). Mammary ultrasounds were performed on d 21, 49, and 70 ($n = 9$ /group) on the rear left and right quarters to quantify PAR and FP areas. Mammary biopsies were collected for histological evaluation of epithelial structures (H&E staining), and to quantify cells positive for ER α (estrogen receptor, α subunit), cell proliferation (Ki67), and apoptosis (TUNEL). Heifer growth from birth to d 49 was similar between CL_{F2} and HT_{F2} for all parameters evaluated. Distances between teats and teat length were not different between groups. On d 70, CL_{F2} tended to have a greater average PAR (right and left quarters) relative to HT_{F2} . Although the left FP was smaller in HT_{F2} relative to CL_{F2} , the average FP was not different. The luminal and non-luminal epithelial structures in the PAR of HT_{F2} were signifi-

cantly smaller than those of CL_{F2} . In addition, HT_{F2} had a reduced percentage of proliferating cells in the epithelial and stromal compartments and a greater percentage of apoptotic cells, particularly in the stroma. The percentage of ER α positive cells was significantly reduced in HT_{F2} . In summary, although HT_{F2} heifer's DMI was similar and they grew at the same rate as CL_{F2} heifers throughout the pre-weaning phase, their mammary glands had smaller PAR areas with fewer epithelial structures characterized by reduced cell turnover and lower ER α expression. These early changes in the microstructure and cellular turnover of the mammary gland may partly explain the reduction in lactation performance relative to CL_{F2} counterparts at maturity.

Key words: In utero, multigenerational, cell turnover

INTRODUCTION

Climate change trends are leading to an increase of heat stress days regardless of geographical location. Consequently, more cattle are exposed to environmental heat stress, regardless of the physiological stage or age of the animals. Exposure of pregnant cows (F_0) to heat stress during the last trimester of gestation negatively impacts their first-generation daughters (F_1), who experienced heat stress in utero. Numerous studies have investigated the detrimental effects of in utero heat stress during late gestation on the F_1 progeny. Even when F_1 heifers are managed as a cohort after birth, those experiencing in utero heat stress showed lower survivability rates, decreased passive transfer of immunity, shorter gestation times, and lower birth weights compared with those born to cows kept cool in late gestation (Dado-Senn et al., 2020; Ouellet et al., 2020; Cattaneo et al., 2022). The negative impacts of intrauterine hyperthermia on growth and development are long-lasting. Indeed, F_1 daughters born to heat-stress cows remain smaller and shorter up to 1 year of age (Monteiro et al., 2016). Further, when these animals reach maturity and enter the lactating herd, they produce significantly less milk in their first lactation, despite having similar mature body weight at calving

Received January 14, 2024.

Accepted March 16, 2024.

*Corresponding author: jlaporta@wisc.edu

relative to their in-utero cooled counterparts (Monteiro et al., 2016; Laporta et al., 2020). One possible explanation for this reduction in first lactation milk yield could be attributed to alterations in mammary gland size, microstructure, and cellular turnover observed in early life (Dado-Senn et al., 2022), some of which persist until their first lactation, 2 years after the prenatal insult occurred (Skibieli et al., 2018). More recently, through retrospective analysis of production records, our group has shown that the reduction in milk yield of F₁ heifers exposed to intrauterine hyperthermia persists through their 2nd and 3rd lactations, indicating a permanent carry-over effect on mammary performance (Laporta et al., 2020). Indeed, a higher culling rate manifests in the second-generation granddaughters (F₂) (Laporta et al., 2020).

Although multigenerational effects are well-studied and extensively documented in other species (Shiota and Kayamura, 1989; Ross et al., 2015; Truong et al., 2023), there's still much to discover and document in dairy cattle. In recent years, there has been a research focus aimed at identifying and characterizing phenotypic differences and understanding the mechanistic link between early-life exposure to environmental heat stress and the long-lasting phenotypes. During the last 2 mo of pregnancy, fetal growth increases exponentially, and maternal exposure to heat stress during this developmental period can “directly” impact the growth and development of F₁ fetal daughters. However, the impact on the F₂ granddaughters is different. The oocytes (female gametes, germline) begin developing in the F₁ fetal daughter, and her entire reserve is present and readily available in the ovaries when she is born (Erickson, 1966). It is thought that late gestation in-utero heat stress could impact the F₂ generation “indirectly” through the fetal daughter germline (Hedhly et al., 2020; Rogers and Phillips, 2021). To date, it is unclear if the reduced milk production at maturity of the F₂ granddaughters (Laporta et al., 2020) is caused by disparities in body size, as a consequence of stunted mammary gland development as observed in F₁ daughters, or both.

To ensure optimal production and herd longevity in the face of climate change, it is becoming more evident that the experiences of previous generations might impact future ones and, therefore, should be considered when selecting replacement animals. This study seeks to characterize the body growth parameters and mammary gland growth trajectories of F₂ granddaughters of cows that were either heat-stressed or cooled during late gestation in a subtropical summer. We hypothesize that F₀ heat stress exposure in late gestation will negatively impact the F₂ generation's growth and mammary development, consistent with our previous observations

in the F₁ daughters. Developing effective strategies to reduce the production losses arising from late-gestation heat stress in dairy cattle requires a deeper understanding of its multigenerational phenotypes and the molecular mechanisms driving it.

MATERIALS AND METHODS

Maternal (F₀) treatments and generation of daughters (F₁) and granddaughters (F₂)

In the summer of 2020, at a commercial dairy farm in Trenton, Florida, pregnant Holstein dams (F₀, granddams, n = 82 blocked by parity, mature-equivalent milk and offspring sire) were exposed to naturally occurring environmental heat stress (HT_{F₀}, shade of a free stall barn, n = 41) or exposed to the same environment but with access to active cooling (CL_{F₀}, fans and water soakers, n = 41) during the last 56 ± 5 d of gestation (i.e., the entire dry period) (Dado-Senn et al., 2021). The first generation of female daughters (F₁, n = 73) born to heat stressed or cooled F₀ dams experienced the treatments via the intrauterine environment (HT_{F₁}, n = 36; CL_{F₁}, n = 37). These daughters, relocated to Arlington Wisconsin, were managed as a cohort from birth until puberty, when they were artificially inseminated using sexed semen from 5 sires balanced between the 2 groups. The F₁ daughters continued to be managed as a cohort during pregnancy until their first calving (Dado-Senn et al., 2021; Davidson et al., 2022) and gave birth to the second generation of female granddaughters (F₂, n = 30, from August to October 2022). The F₂ heifers were exposed to their granddam's heat-stressed or cooling treatments in utero indirectly through the F₁ fetal daughter germline. No treatment was applied to the F₂ generation. These groups will be referred to as HT_{F₂} (n = 12) and CL_{F₂} (n = 18).

Management of granddaughters (F₂) from birth to weaning

The F₂ granddaughters were raised in individual sand-bedded polyethylene calf hutches (Calf-Tel, L. T. Hampel Corp.) at the University of Wisconsin-Madison Arlington Agricultural Research Station. All heifers received colostrum (average BRIX 26%) within 4 h of birth. Afterward, all heifers received whole pasteurized milk in 2 daily meals (2 quarts/meal the first 2 d of life, 3 quarts/meal from 3 to 14 d, and 4 quarts/meal from 15 to 42 d). At 42 d, milk was decreased incrementally and ceased at 49 d. Health was monitored daily by the farm staff, and all heifers were treated according to farm standard operating protocols by trained veterinarians. Starter (VitaPlus medicated 18% crude protein,

5.2% fat, **Table 1**) was offered ad libitum beginning at birth, and intake was monitored from 28 d through 56 d. At 56 d, all heifers were moved to a 4-calf super-hutch (Caft-Tel, L. T. Hampel Corp.) until 12 wk of age. All heifers were transitioned to a grower grain at this stage, and individual intake was not monitored.

Whole-body growth and mammary gland measurements

At 1, 7, 21, 35, 49, and 70 d old, hip height, withers height, chest girth, head circumference, and body weight were measured. Hip height (i.e., ground to hook) and wither height (i.e., ground to top of wither) were measured using a tape measure. Chest (heart) girth was measured with a soft tape measure directly behind the front legs and around the body, and head circumference was measured around the head in front of the ears with a soft tape measure. Body weight was measured using a calf cart with a built-in scale. At 21, 49, and 70 d old, mammary ultrasounds (Mindray Z60, Shenzhen, China) were performed using a convex probe. Heifers were in a standing position at 21 and 49 d, where all 4 quarters were imaged. At 70 d, a subset of heifers' (n = 8–10 per treatment) left and right rear quarters were scanned with a convex probe in the supine position where visible parenchyma and fat pad were captured. The probe depth was set at 2.8 for all calves, and the visible parenchyma and fat pad were captured in a 4-s video for each quarter. The probe was placed directly behind the teat, the gland cistern was located, and the video was captured. At d 21, 35, 39, and 70, measures of teat length (base of the teat to the tip) and distance between teats (center of teat base to center of teat base) were recorded using calipers. Individual frames from each video were isolated, and the frame with the greatest visible parenchyma area was chosen for each animal at each time point evaluated. The surface areas of parenchyma and fat pad tissue were measured using Q-Path version 0.4.3 (Bankhead et al., 2017). Pixels² were converted to mm² in Excel (Microsoft).

Mammary gland biopsies and histological analysis

At 70 ± 5 d of age, post-weaning mammary biopsies were performed on a subset of heifers (n = 6 per group). Briefly, all heifers were given intravenous Xylazine (AnaSed, Lloyd Inc., Iowa) at 0.02 mg/kg and placed in the supine position. The mammary gland parenchyma was palpated, and 2 mL of lidocaine (Clipper Distributing Company, Missouri) was administered into the gland. All biopsies were taken from the rear right gland quarter. Using a #15-scalpel blade, a small incision was made, and a 2 mm biopsy punch (Integra

Table 1. Nutritional content of the starter grain concentrate offered at libitum to Holstein dairy heifers from birth to 70 d. of age

	Mean ¹	SD
Moisture (%)	9.75	0.45
Dry Matter (%)	90.25	0.45
<i>Nutrient Content (DM Basis)</i>		
CP (%)	22.0	0.6
Fat (%)	4.14	0.4
ADF (%)	11.0	0
aNDF (%)	17.5	0.7
NFC (%)	51.0	0.05
Ash (%)	6.13	0.545
ME (Mcal/kg)	2.99	0.01
Ca (%)	1.16	0.09
P (%)	0.585	0.015
Mg (%)	0.25	0
K (%)	1.36	0.04
Na (%)	0.255	0.005
Fe (PPM)	155.5	7.5
Mn (PPM)	62.0	6
Zn (PPM)	119.5	0.5
Cu (PPM)	27.5	0.5

¹Averaged (Mean ± Standard Deviation) chemical analysis of grain samples taken during experimental period.

Miltex #33–31) was inserted and twisted in a clockwise motion to cut and collect the tissue. After the procedure, Flunixin Meglumine (Flunazine, Bimeda, Illinois) was administered intravenously at a 1.6 mg/kg dose. The PAR tissue (~20–60 mg) was washed in cold PBS, placed in tissue cassettes, and stored in 10% NBF (Neutral Buffered Formalin) for 18–20 h. The tissue was paraffin-embedded, sectioned at 5 µm, and stained with H&E to visualize the architecture of the epithelial structures. Additional sections were used to assess cellular turnover and estrogen receptor α (ERα) via immunohistochemistry and immunoperoxidase procedures. Briefly, Ki-67 antibody (Mouse anti-Human Ki67, SAKO #M7240, clone MIB-1) was used to quantify cellular proliferation. To evaluate cell death, the TUNEL method was used with the ApopTag Peroxidase In Situ Apoptosis Detection Kit (Millipore Sigma #s7100) according to the manufacturer's protocol. To evaluate ERα, sections were incubated with mouse monoclonal ERα primary antibody (1:100, Santa Cruz Biotechnology #C-311sc787) for one hour with stain visualization using Mach 2 Mouse HRP polymer (Biacare Medical, #MHRP520L).

Tissue images were captured using a brightfield microscope (Keyence BX800, Keyence Corporation of America, Osaka, Japan). Five random photomicrographs were taken per animal per stain. The H&E-stained mammary sections were used to determine the area of epithelial structures which were classified into either luminal (presence of a hollow lumen) or non-luminal structures (no visible lumen). Using Image J, the areas were quantified by tracing closely around the

mammary epithelial structures. The Ki-67 antibody was used to determine the percent of proliferating cells, and the TUNEL assay was used to determine the percent of apoptotic cells. The total number of cells per photomicrograph were counted using BX-800 Keyence Analyzer software (Keyence Corporation of America, Osaka, Japan), and positive cells were hand-counted in image J. The number of cells by epithelial and stroma cell compartments was counted and analyzed separately.

Statistical analyses

All statistical analysis was performed using the statistical software SAS (SAS Institute Inc., Cary, NC). Repeated measures of calf body and mammary growth, feed intake, and efficiency were analyzed through ANOVA using the MIXED procedure. The model for growth (BW, HH, WH, CG, HC) and ultrasonography at 21 and 49 d included fixed effects of maternal F₀ treatment (TRT), time (d), and their interaction. Animal (ID) within TRT was used as a random effect. Ultrasonography and epithelial structure data collected at 70 d were analyzed with TRT as a fixed effect and ID as a random effect. The GLIMMIX procedure was used to analyze cell proliferation, apoptosis, and ER α count data. The model evaluated the ratio of total positively stained cells to total cells for each tissue cell type, with TRT as the fixed effect and ID within replicate as a random effect. All residuals were tested for normality. Box-Cox was used to determine which transformation was necessary if normality was unmet. The mammary luminal epithelial areas were log-transformed based on Box-Cox lambda. The Least Square Means \pm standard error is presented unless noted otherwise. A *P*-value ≤ 0.05 was considered statistically significant, and *P*-values > 0.05 and ≤ 0.10 were considered tendencies.

RESULTS

Whole-body growth and mammary gland macrostructural outcomes are presented in **Table 2**. There were no significant effects of the F₀ treatment or interactions for the whole-body and macrostructural mammary growth parameters evaluated in the F₂ generation (*P* > 0.12). A main effect of day was observed for all variables (*P* < 0.01), reflecting a similar age-related growth trajectory for all heifers through the first 10 weeks of life (d 1- 70).

Mammary ultrasound outcomes evaluated at d 21 and 49 are presented in **Table 3**. For all the parameters analyzed via ultrasound, there were no significant effects of the maternal treatment or significant interactions (*P* > 0.25). However, an effect of the day was

observed (*P* < 0.04), whereby the visible parenchyma and fat pad areas increased from d 21 to 49.

Outcomes related to PAR epithelial structures and ER α cells are shown in **Figure 1**. The PAR tissue of CL_{F₂} had greater non-luminal and luminal structure areas than HT_{F₂} (**Figure 1b**; non-luminal: 23,386 \pm 1,738 vs. 16,789 \pm 1,570 μm^2 *P* = 0.005; luminal: 71,125.41 \pm 8,443 vs 48,484.53 \pm 3,556 μm^2 *P* = 0.006 for CL_{F₂} and HT_{F₂}, respectively). The percent of ER α positive cells was greater in the PAR epithelial compartment of CL_{F₂} when compared with that of HT_{F₂} (**Figure 1d**; 53.5% \pm 3.3 vs. 40.0% \pm 2.7; *P* = 0.0033). The percent of ER α positive cells did not differ between groups in the PAR stromal compartment.

Mammary gland cell turnover, cell proliferation, and cell death, outcomes are shown in **Figure 2**. Granddaughters of in utero CL_{F₁} had a higher percentage of proliferating cells in both the PAR epithelial (**Figure 2b**; 10.6% \pm 1.1 vs. 7.8% \pm 0.80 for CL_{F₂} and HT_{F₂} respectively, *P* = 0.04) and stromal tissue compartments (**Figure 2b**; 7.3% \pm 1% vs. 4.2% \pm 0.6 for CL_{F₂} and HT_{F₂} respectively, *P* = 0.004). Cell proliferation percentages were greater in the CL_{F₂} heifers when analyzing the total cell population (**Figure 2b**; 8.7% \pm 0.7 vs. 5.5% \pm 0.6 for CL_{F₂} and HT_{F₂} respectively, *P* = 0.003). Conversely, the percentage of apoptotic cells in the stromal compartment, and the total percentage of apoptotic cells were greater in the PAR of HT_{F₂} granddaughters than CL_{F₂} granddaughters (**Figure 2d**; Stromal: 0.33% \pm 0.07 vs. 0.62% \pm 0.08 *P* = 0.009; Total: 0.27% \pm 0.03 vs. 0.43% \pm 0.04 *P* = 0.003 for CL_{F₂} and HT_{F₂} respectively). There was no difference in the percentage of apoptotic cells in the PAR epithelial compartment.

Outcomes related to mammary gland ultrasonography collected at d 70 are presented in **Figure 3**. Visible parenchyma area was greater in CL_{F₂} heifers compared with HT_{F₂} for the right rear quarter (**Figure 3c**; Right: 2,771.03 + 253.41 vs 1,885.98 + 283.32 mm^2 *P* = 0.045) as well as the average of the right and left rear quarters (average: 2793.9 \pm 222.6 vs 2097.6 \pm 236.1 *P* = 0.05). There were no differences in the visible parenchyma areas of the left rear quarters (*P* > 0.42). There were no differences in the visible fat pad of the right rear quarters nor the average of the right and left rear quarters combined (*P* > 0.12). However, CL_{F₂} heifers had a greater visible fat pad area of the left rear quarter than HT_{F₂} (4593.6 \pm 383.3 vs. 3366.0 \pm 428.51 *P* = 0.05).

DISCUSSION

This is the first study to assess macrostructural and microstructural phenotypes in the second generation (F₂, granddaughters) of dairy cows undergoing heat

Larsen and Laporta: PRENATAL HEAT STRESS ON F₂'S MAMMARY GROWTH**Table 2.** Heifer's growth trajectory, feed intake, and mammary gland macrostructural teat measures, during the preweaning period

Item	Treatment ¹			<i>P</i> -value		
	CL _{F2}	HT _{F2}	SEM ²	TRT	Days ³	TRT × Days
Starter Intake (kg/day)	1.25	1.15	0.06	0.27	<0.01	0.38
Average Daily Gain (kg/day)	0.80	0.78	0.02	0.50	—	—
Calf Growth						
Body Weight (kg)	55.1	56.1	0.98	0.49	<0.01	0.58
Hip Height (cm)	86.8	87.8	0.51	0.18	<0.01	0.61
Wither Height (cm)	84.2	85.2	0.61	0.24	<0.01	0.25
Chest Girth (cm)	86.5	86.6	0.48	0.86	<0.01	0.89
Head Circumference (cm)	55.1	55.4	0.42	0.65	<0.01	0.77
Mammary Gland Teat						
<i>Average Length</i> (mm)						
Front Teats	9.96	10.0	0.60	0.94	<0.01	0.69
Rear Teats	9.34	9.17	0.33	0.69	<0.01	0.64
<i>Distance Between</i> (mm)						
Front Teats	32.7	33.2	1.74	0.85	<0.01	0.17
Rear Teats	20.2	21.3	0.69	0.26	<0.01	0.12
Left Teats	23.5	23.3	1.08	0.91	<0.01	0.79
Right Teats	23.2	23.1	1.10	0.94	<0.01	0.79

¹Overall treatment (TRT) estimates. TRT = CL_{F2} = granddaughter (F₂, second generation) of cooled granddams (F₀ exposed to heat stress with access to shade, fans, and water soakers) for the last 56 d of gestation of the F₁ (first generation), HT_{F2} = granddaughter of heat-stressed granddams (heat stress with access to shade only).

²Average of SEM from both treatments.

³Days = 1, 7, 21, 35, 49, 70 d of age for calf growth; 21, 35, 49, and 70 for mammary growth measures.

stress during late gestation. A key finding is that the F₂ granddaughters born to heat-stressed granddams do not manifest the classic growth retardation hall-

marks observed in utero heat-stressed F₁ daughters (i.e., reduced birth weight and stature; Monteiro et al., 2016). Additionally, phenotypic mammary gland

Table 3. Quantification of mammary gland parenchyma and fat pad areas via ultrasonography at 21 and 49 d old Holstein heifers

Item	Treatment ¹			<i>P</i> -value		
	CL _{F2}	HT _{F2}	SEM ²	TRT	Day	TRT × Day
Pre-weaned Period ^{3,4}						
Parenchyma Area (mm ²)						
Left Front ⁵	588	629	68	0.68	<0.01	0.98
Left Rear	622	658	80	0.75	<0.01	0.82
Right Front	630	647	78	0.88	<0.01	0.70
Right Rear	643	714	75	0.51	<0.01	0.94
Average Front	610	638	64	0.77	<0.01	0.83
Average Rear	637	685	69	0.63	<0.01	0.87
Average All	624	661	64	0.69	<0.01	0.83
Fat Pad Area (mm ²)						
Left Front	1098	1268	147	0.42	0.03	0.34
Left Rear	1255	1562	194	0.28	<0.01	0.16
Right Front	1370	1397	194	0.92	<0.01	0.13
Right Rear	1375	1503	158	0.57	0.04	0.92
Average Front	1239	1334	127	0.61	<0.01	0.59
Average Rear	1306	1531	135	0.25	<0.01	0.36
Average All	1264	1435	119	0.32	<0.01	0.45

¹Overall treatment (TRT) estimates. TRT = CL_{F2} = granddaughter (F₂, second generation) of cooled granddams (F₀ exposed to heat stress with access to shade, fans, and water soakers) for the last 56 d of gestation of the F₁ (first generation), HT_{F2} = granddaughter of heat-stressed granddams (heat stress with access to shade only).

²SEM average from both treatments.

³Analysis of ultrasound images taken at d 21 and d 49.

⁴Ultrasound videos were taken from the front and rear right and left mammary gland quarters.

macrostructural differences were not observed between HT and CL F₂ granddaughters, as previously reported for CL and HT F₁ daughters (i.e., shorter teat length and distance; Dado-Senn et al., 2022). However, despite their unimpacted whole-body and macrostructural mammary growth trajectory, the mammary gland epithelial microstructure and cellular turnover of HT_{F₂}'s are significantly stunted. The findings of this study are relevant to the dairy industry, as farmers often rely on pre-established body weight and stature benchmarks to make culling and replacement decisions. Despite having lower production potential, HT_{F₂} faces the same risk of being culled as CL_{F₂}. The lack of phenotypic differences between F₂ heifers born to in utero HT_{F₁} or CL_{F₁}'s highlights a critical pitfall in the management of multi-generationally impacted heat-stressed animals, as HT_{F₂} heifers will pass through herd checkpoints while their mammary glands are programmed to perform at sub-optimal levels, ultimately affecting milk production.

The first-generation CL_{F₁} daughters are heavier and taller than HT_{F₁} daughters through one year of age, around the time of breeding (Monteiro et al., 2016). This disparate growth rate is not observed in the second generation of HT_{F₂} granddaughters, where growth rates are identical to CL_{F₂} counterparts. This could mean that the HT_{F₂} granddaughters were able to overcome the growth challenge their mothers (in utero exposed F₁) faced due to more direct exposure to hyperthermia as a developing fetus. Conversely, the resulting F₂ heifers evaluated herein were exposed as a germ cell developing inside the fetal F₁ daughters at the time of maternal F₀ heat stress exposure. Therefore, the effect of hyperthermia might have been less exacerbated for the developing egg relative to the whole fetus. Yet, CL_{F₂} granddaughters have longer, thinner hair coats and fewer but larger sebaceous glands than HT_{F₂} granddaughters (Davidson et al., 2023). These differences may indicate that some phenotypic differ-

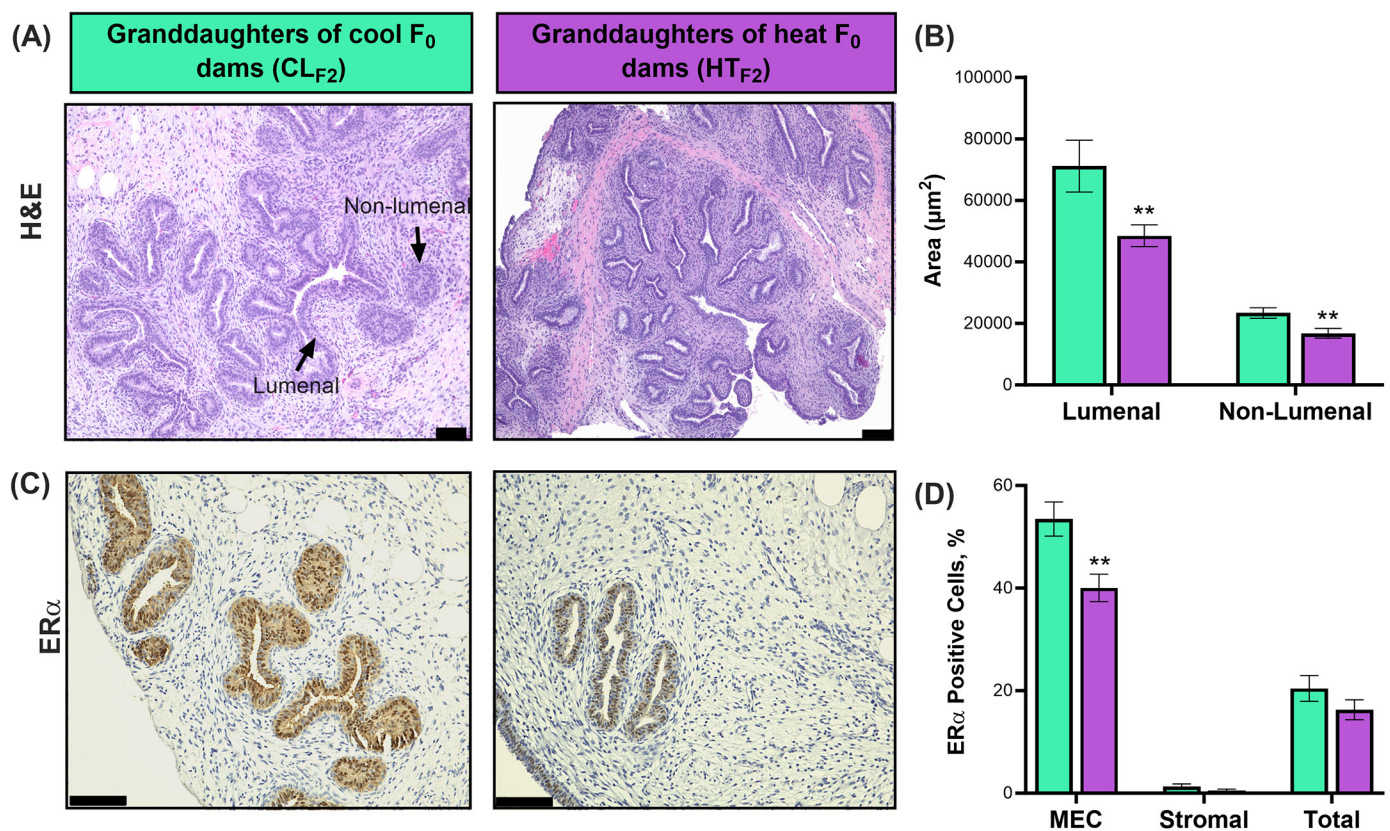


Figure 1. Histological and immune-histological evaluation of mammary gland parenchyma microstructure (H&E staining) and estrogen receptor α (ER α monoclonal antibody). Second-generation heifers (granddaughters, F₂) were born to first-generation (daughters, F₁) cows that were heat-stressed or cooled in-utero (HT_{F₁} and CL_{F₁}, respectively) during late gestation (last 56 \pm 5 d). Mammary biopsies were collected from CL_{F₂} (n = 6) and HT_{F₂} (n = 6) granddaughters at 70 d of age. **(A)** Histological microphotographs of H&E-stained slides were taken at 10x, scale = 100 μ m. **(B)** The area of luminal (visible lumen) and non-luminal (no visible lumen) epithelial structures were quantified in image J. **(C)** Histological microphotographs of ER α expression were taken at 20x, scale = 100 μ m. **(D)** The percent of mammary epithelial cells (MEC), stromal cells, and total cells (MEC + stromal) positive for ER α were counted using BX-800 Keyence Analyzer. Data are presented as LSM \pm SEM. Arrows indicate luminal and non-luminal epithelial structures. Asterisk (*) represents $P < 0.05$, (**) represents $P < 0.01$.

ences exist between these animals, potentially indicating different thermoregulatory capacities arising from germline exposure to hyperthermia.

By evaluating mammary gland parenchyma tissue size via ultrasonography combined with histological assessments, we begin to unravel hidden carry-over effects of late-gestation heat stress in the F₂ generation. These alterations in mammary microstructure and cellular turnover, along with the reduced ER α , may lead to a slower mammary growth rate in response to estrogen at puberty, resulting in reduced milk synthetic capacity and lactation outcomes at maturity. Ultrasonography allows the visualization of the growing mammary gland parenchyma tissue without requiring terminal studies to harvest the glandular structures and dissect specific types of tissues post-harvest. Although there were no differences between groups in visible parenchyma or fat pad surface areas in the pre-weaned period (assessed at 21 and 49 d of age), these differences arise as the heifers begin to develop their mammary glands allometrically. It has previously been thought that the onset of al-

lometric growth did not occur until puberty (Tucker, 1987), however, recent studies have shown a shift in this dogma, highlighting the importance of assessing pre-pubertal mammary growth while also introducing this period as a time of allometric growth (Sørensen et al., 1987; Geiger et al., 2016; Soberon and Van Amburgh, 2017) Additionally, our group has shown that PAR mass increases about 25-fold from birth to weaning (Dado-Senn et al., 2022) The lack of differences at earlier time points could be attributed to the sensitivity of the ultrasound or the standing position at which these measures were taken compared with the supine position which may increase visible surface area of the gland. Regardless, the ongoing development of more refined quantification methods and ultrasound technologies is expected to allow for an earlier assessment and detection of PAR growth differences among animals. In the present study, mammary gland ultrasounds performed at 10 weeks old revealed that CL_{F2} granddaughters had greater average parenchyma surface area in the rear quarters. This could indicate a greater rate of growth

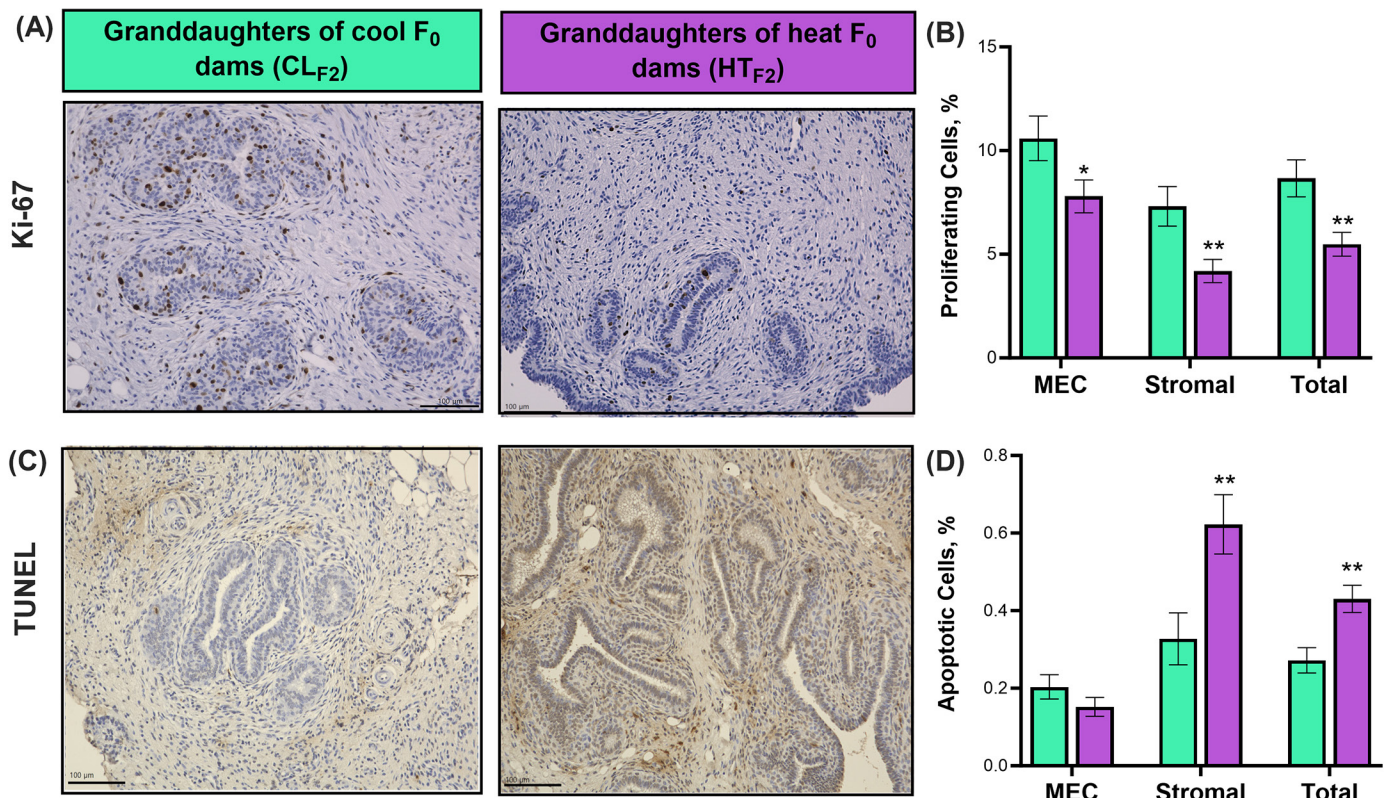


Figure 2. Immunohistochemistry evaluation for cellular proliferation (Ki-67) and cell death (TUNEL) in the mammary gland of 70 d old Holstein heifers. Second-generation heifers (granddaughters, F₂) were born to first-generation (daughters, F₁) cows that were heat-stressed or cooled in-utero (HT_{F1} and CL_{F1}, respectively) during late gestation (last 56 ± 5 d). **(A, C)** Histological microphotographs of proliferating (Ki-67-positive cells) and apoptotic (TUNEL-positive). Percent of cells mammary epithelial cells (MEC), stromal cells, and total cells (MEC + stromal) undergoing proliferation **(B)** or apoptosis **(D)**. Total cells were counted using BX-800 Keyence Analyzer, and Ki-67 and TUNEL-positive cells were hand-counted. Data are presented as LSM ± SEM. Asterisk (*) represents $P < 0.05$, (**) represents $P < 0.01$.

and development compared with that of HT_{F₂} granddaughters. Notably, the images extracted from the ultrasound videos had similar developmental characteristics as those reported in a recent study, where calves also at 10 weeks of age had visible parenchyma in an oval shaped structure with some apparent developing ductal structures (Seibt et al., 2023). The lack of difference in PAR between groups evaluated before 6 weeks of age may have been due to the younger age of the animal and the overall smaller PAR mass due to growth rates at this time. This observation is consistent with Seibt et al. (2023), who found that most heifers had little to no visible parenchyma area until they reached 8 weeks old.

To further evaluate the development of the mammary glands in these heifers, a mammary biopsy was

collected at 70 d of life to assess the microstructure and cellular makeup. We quantified the area of the ductal epithelial structures via H&E staining, revealing that CL_{F₂} granddaughters had larger luminal (structures with a single layer of mammary epithelial cells with a hollow lumen formed) and non-luminal (structures with mammary epithelial cells but no hollow lumen) epithelial structures. This is consistent with data from their mothers (CL_{F₁}) PAR harvested at a similar age, where luminal structures were significantly larger than their HT_{F₁} counterparts (Dado-Senn et al., 2022). An interesting observation of the present study is the larger total area of the non-luminal structures of HT_{F₂} heifers. This observation, along with smaller luminal-epithelial structures manifesting lower cell proliferation, possibly reflects a delayed developmental progression of the ru-

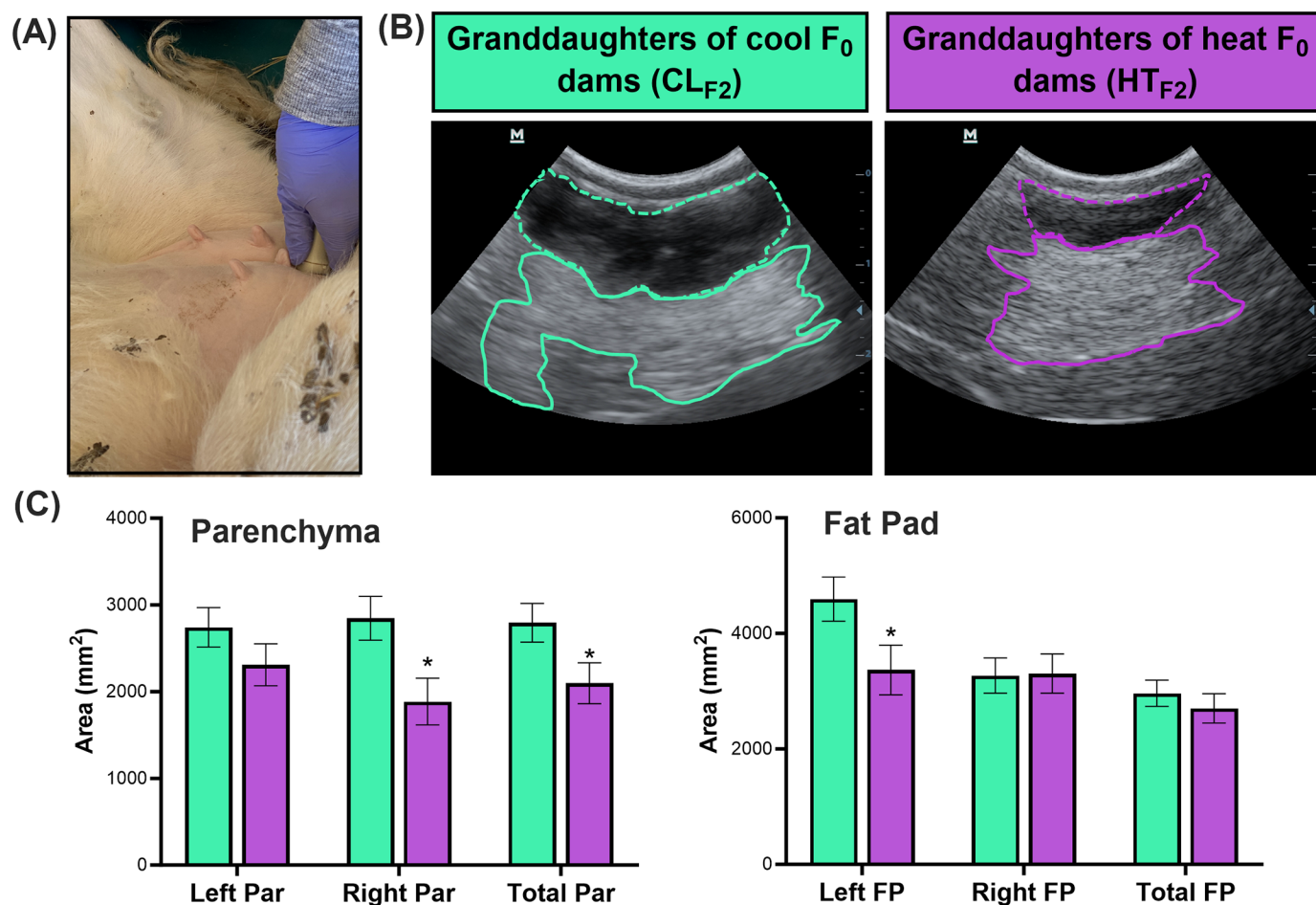


Figure 3. Ultrasonographic analysis of heifer's mammary glands. Second-generation heifers (granddaughters, F₂) were born to first-generation (daughters, F₁) cows that were heat-stressed or cooled in-utero (HT_{F₁} and CL_{F₁}, respectively) during late gestation (last 56 ± 5 d). Mammary ultrasounds were performed in CL_{F₂} (n = 9) and HT_{F₂} (n = 8) granddaughters at 70 d of age. (A) Representative photo of the position of the ultrasound probe in the rear quarter relative to the teat at the time of video imaging. (B) Ultrasonographic photos of visible mammary parenchyma (PAR, dotted highlighted areas) and fat pad (FP, solid highlighted areas) for CL_{F₂} (green) and HT_{F₂} (purple). (C) Quantification of parenchyma and fat pad area in left, right, and average of left and right quarters calculated using Q-path Software. Asterisk (*) represents *P* < 0.05.

dimentary ductal tree within the smaller PAR tissue of the mammary gland of HT_{F2} heifers. Interestingly, the stunted development of ductal-epithelial structures in the PAR tissue is conserved through at least 2 generations of heifers, daughters, and granddaughters. This is the first study to report a multigenerational perpetuation of mammary gland microstructural alterations arising from late-gestation heat exposure.

Estrogen receptor α (ER α) plays a large role in the formation of ductal structures, especially during the early phases of allometric mammary gland growth and development. In the present study, although ER α is present and is expressed in both groups of heifers, there is significantly less expression in the HT_{F2} mammary epithelial cell compartment relative to CL_{F2}. This finding, combined with the overall smaller luminal epithelial structures, may reflect a delayed developmental progression of ductal structures as a result of the heat stress insult experienced by their F₀ grandmothers impacting their F₁ mothers and their germline in utero (Li and Capuco, 2008). Other groups have identified ER α as a regulator of estrogen-responsive genes in the bovine. One study has reported that the amount of proliferating cells decreased due to lack of ER α , however no differences in apoptosis were reported (Mallepell et al., 2006). In this study, CL_{F2} granddaughters had a greater percentage of proliferating cells, and a lower percentage of cells undergoing apoptosis compared with the HT_{F2} granddaughters. Exposure to high temperatures can cause cell death in the bovine mammary epithelial gland cells (Wohlgemuth et al., 2016; Chen et al., 2020). This suggests that the HT_{F2} granddaughters' impaired proliferation could be a consequence of decreased ER α expression, presumably from the heat stress insult, and the increased apoptosis may be a more direct programming effect from the heat-stressed germ cell in the fetal F₁ daughter or via another unknown mechanism not evaluated herein. Programming for higher cell death due to heat stress is a disadvantage because there may be less capacity for mammary and ductal development. Further research is necessary to understand the underlying molecular mechanisms driving the observed changes and whether heat stress during other gestation periods (i.e., early and mid-gestation) would trigger similar multigenerational effects in dairy cattle. It is imperative that we continue to investigate how heat stress impacts the fetal germline to better understand how to prevent and rescue the negative hidden effects of heat stress in these animals before there is a loss of production.

CONCLUSIONS

The naturally occurring environmental conditions of the subtropical climates in the southeastern U.S., characterized by chronic periods of high temperature and humidity, can lead to chronic heat stress in dairy cattle resulting in long-lasting damage to the production potential of multiple generations. Providing active cooling can effectively dissipate accumulated heat under these conditions, allowing the pregnant F₀ dam to maintain thermoneutrality while her F₁ daughter is developing in utero. In addition, the thermal environment in which the female germ line (that will give rise to the F₂ granddaughters) undergoes the last stages of development is critical. Despite CL_{F2} and HT_{F2} having identical growth trajectories, dry matter intakes, and phenotypic anatomy of the mammary gland, CL_{F2} heifers develop larger parenchyma mass, with more developed ductal-epithelial structures, greater expression of ER α , and higher rates of proliferation. There seem to be hidden multigenerational effects of late-gestation heat stress that contribute to HT_{F2} heifers "passing under the radar," leading to cows entering the lactating herd at a disadvantage, ultimately leaving less milk in the bulk tank.

ACKNOWLEDGMENTS

We thank the University of Wisconsin–Madison's Emmons Blaine Dairy Cattle Center staff and veterinarians for their assistance in animal management. Further acknowledgment goes to the current and former graduate students, Brittney Davidson, Bethany Dado-Senn, Emily Tabor, Sena Field, Kaylee Riesgraf, and Anne Guadagnin, who assisted with animal rearing and data collection. This study was partially funded by USDA-NIFA AFRI Foundational Program Award 2019-67015-29445.

Competing Interests The authors declare no competing interests

REFERENCES

- Bankhead, P., M. B. Loughrey, J. A. Fernández, Y. Dombrowski, D. G. McArt, P. D. Dunne, S. McQuaid, R. T. Gray, L. J. Murray, H. G. Coleman, J. A. James, M. Salto-Tellez, and P. W. Hamilton. 2017. QuPath: Open source software for digital pathology image analysis. *Sci. Rep.* 7:16878. <https://doi.org/10.1038/s41598-017-17204-5>.
- Cattaneo, L., J. Laporta, and G. E. Dahl. 2022. Programming effects of late gestation heat stress in dairy cattle. *Reprod. Fertil. Dev.* 35:106–117. <https://doi.org/10.1071/RD22209>.
- Chen, K. L., H. L. Wang, L. Z. Jiang, Y. Qian, C. X. Yang, W. W. Chang, J. F. Zhong, and G. D. Xing. 2020. Heat stress induces apoptosis through disruption of dynamic mitochondrial networks in dairy cow mammary epithelial cells. *In Vitro Cell. Dev. Biol. Anim.* 56:322–331. <https://doi.org/10.1007/s11626-020-00446-5>.

Larsen and Laporta: PRENATAL HEAT STRESS ON F2'S MAMMARY GROWTH

- Dado-Senn, B., S. L. Field, B. D. Davidson, L. T. Casarotto, M. G. Marrero, V. Ouellet, F. Cunha, M. A. Sacher, C. L. Rice, F. P. Maunsell, G. E. Dahl, and J. Laporta. 2021. Late-Gestation in utero Heat Stress Limits Dairy Heifer Early-Life Growth and Organ Development. *Front. Anim. Sci.* 2:750390. <https://doi.org/10.3389/fanim.2021.750390>.
- Dado-Senn, B., J. Laporta, and G. E. Dahl. 2020. Carry over effects of late-gestational heat stress on dairy cattle progeny. *Theriogenology* 154:17–23. <https://doi.org/10.1016/j.theriogenology.2020.05.012>.
- Dado-Senn, B. M., S. L. Field, B. D. Davidson, G. E. Dahl, and J. Laporta. 2022. In utero hyperthermia in late gestation derails dairy calf early-life mammary development. *J. Anim. Sci.* 100:skac186. <https://doi.org/10.1093/jas/skac186>.
- Davidson, B. D., E. T. Gonzales, G. L. Mast, and J. Laporta. 2023. Late-gestation heat stress in Holstein dams programs in utero development of daughter's germline, triggering skin and hair morphology adaptations of granddaughters. *JDS Commun.* 5:83–88. <https://doi.org/10.3168/jdsc.2023-0400>.
- Davidson, B. D., K. M. Sarlo Davila, R. G. Mateescu, G. E. Dahl, and J. Laporta. 2022. Effect of in utero exposure to hyperthermia on postnatal hair length, skin morphology, and thermoregulatory responses. *J. Dairy Sci.* 105:8898–8910. <https://doi.org/10.3168/jds.2022-22202>.
- Erickson, B. H. 1966. Development and senescence of the postnatal bovine ovary. *J. Anim. Sci.* 25:800–805. <https://doi.org/10.2527/jas1966.253800x>.
- Geiger, A. J., C. L. M. Parsons, R. E. James, and R. M. Akers. 2016. Growth, intake, and health of Holstein heifer calves fed an enhanced preweaning diet with or without postweaning exogenous estrogen. *J. Dairy Sci.* 99:3995–4004. <https://doi.org/10.3168/jds.2015-10405>.
- Hedhly, A., A. Nestorova, A. Herrmann, and U. Grossniklaus. 2020. Acute heat stress during stamen development affects both the germline and sporophytic lineages in *Arabidopsis thaliana* (L.) Heynh. *Environ. Exp. Bot.* 173:103992. <https://doi.org/10.1016/j.envexpbot.2020.103992>.
- Laporta, J., F. C. Ferreira, V. Ouellet, B. Dado-Senn, A. K. Almeida, A. De Vries, and G. E. Dahl. 2020. Late-gestation heat stress impairs daughter and granddaughter lifetime performance. *J. Dairy Sci.* 103:7555–7568. <https://doi.org/10.3168/jds.2020-18154>.
- Li, R. W., and A. V. Capuco. 2008. Canonical pathways and networks regulated by estrogen in the bovine mammary gland. *Funct. Integr. Genomics* 8:55–68. <https://doi.org/10.1007/s10142-007-0055-6>.
- Mallepell, S., A. E. Krust, P. Chambon, and C. Briskin. 2006. Paracrine signaling through the epithelial estrogen receptor is required for proliferation and morphogenesis in the mammary gland. *Proc. Natl. Acad. Sci. USA* 103:2196–2201. <https://doi.org/10.1073/pnas.0510974103>.
- Monteiro, A. P. A., S. Tao, I. M. T. Thompson, and G. E. Dahl. 2016. In utero heat stress decreases calf survival and performance through the first lactation. *J. Dairy Sci.* 99:8443–8450. <https://doi.org/10.3168/jds.2016-11072>.
- Ouellet, V., J. Laporta, and G. E. Dahl. 2020. Late gestation heat stress in dairy cows: Effects on dam and daughter. *Theriogenology* 150:471–479. <https://doi.org/10.1016/j.theriogenology.2020.03.011>.
- Rogers, A. K., and C. M. Phillips. 2021. RNAi pathways repress reprogramming of *C. elegans* germ cells during heat stress. *Nucleic Acids Res.* 48:4256–4273. <https://doi.org/10.1093/nar/gkaa174>.
- Ross, J. W., B. J. Hale, N. K. Gabler, R. P. Rhoads, A. F. Keating, and L. H. Baumgard. 2015. Physiological consequences of heat stress in pigs. *Anim. Prod. Sci.* 55:1381–1390. <https://doi.org/10.1071/AN15267>.
- Seibt, K. D., T. Scheu, C. Koch, M. H. Ghaffari, and H. Sauerwein. 2023. Ultrasound characterization of mammary gland development in heifer calves fed at two different levels until weaning. *Anat. Histol. Embryol.* 52:500–511. <https://doi.org/10.1111/ahc.12907>.
- Shiota, K., and T. Kayamura. 1989. Effects of Prenatal Heat Stress on Postnatal Growth, Behavior and Learning Capacity in Mice. *Neonatology* 56:6–14. <https://doi.org/10.1159/000242981>.
- Skibieli, A. L., F. Peñagaricano, R. Amorín, B. M. Ahmed, G. E. Dahl, and J. Laporta. 2018. In Utero Heat Stress Alters the Offspring Epigenome. *Sci Rep* 8. doi:<https://doi.org/10.1038/s41598-018-32975-1>.
- Soberon, F., and M. E. Van Amburgh. 2017. Effects of preweaning nutrient intake in the developing mammary parenchymal tissue. *J. Dairy Sci.* 100:4996–5004. <https://doi.org/10.3168/jds.2016-11826>.
- Sørensen, M. T., K. Sejrsen, and J. Foldager. 1987. Estimation of Pubertal Mammary Development in Heifers by Computed Tomography. *J. Dairy Sci.* 70:265–270. [https://doi.org/10.3168/jds.S0022-0302\(87\)80006-1](https://doi.org/10.3168/jds.S0022-0302(87)80006-1).
- Truong, L., M. R. Miller, R. D. Sainz, and A. J. King. 2023. Changes in Japanese quail (*Coturnix coturnix japonica*) blood gases and electrolytes in response to multigenerational heat stress. *PLOS Climate* 2:e0000144. <https://doi.org/10.1371/journal.pclm.0000144>.
- Tucker, H. A. 1987. Quantitative Estimates of Mammary Growth During Various Physiological States: A Review. *J. Dairy Sci.* 70:1958–1966. [https://doi.org/10.3168/jds.S0022-0302\(87\)80238-2](https://doi.org/10.3168/jds.S0022-0302(87)80238-2).
- Wohlgemuth, S. E., Y. Ramirez-Lee, S. Tao, A. P. A. Monteiro, B. M. Ahmed, and G. E. Dahl. 2016. Short communication: Effect of heat stress on markers of autophagy in the mammary gland during the dry period. *J. Dairy Sci.* 99:4875–4880. <https://doi.org/10.3168/jds.2015-10649>.

ORCID

Grace. A. Larsen  <https://orcid.org/0009-0005-8839-8555>
 Jimena Laporta  <https://orcid.org/0000-0002-3186-5360>